

Near-Net-Shape Forming of Metallic Bipolar Plates for Planar Solid Oxide Fuel Cells by Induction Plasma Spraying

R. Henne, M. Müller, E. Proß, G. Schiller, F. Gitzhofer, and M. Boulos

(Submitted 13 March 1998; in revised form 14 October 1998)

In one of the present designs of solid oxide fuel cells (SOFC), metallic bipolar plates with gas channels on the surface are used, which consist of a chromium alloy and are manufactured by a time consuming and costly multistep process. To reduce the production time and costs, attempts were made to develop an alternative near-net-shape production method based on RF-induction plasma spray technology. With this process raw powders, as applied for the “conventional” sintering route as well as recycled powders from used bipolar plates, have been applied. The process parameters were adapted to both powders, and the obtained products were qualified. The near-net-shape production requires the formation of a gas channel structure already with the spray process using structured substrates. Therefore, different spray angles occur during the deposition process. The influence of the spray angle on the microstructure of the free-standing parts was investigated. The required gas tightness for grooved profiles with relatively large channel depths and widths can only be achieved using spray angles between 90° and approximately 60° . Then a tilting of the substrate and an adapted design of the gas channel profiles are needed to fulfill the structural requirements for the bipolar plates.

Keywords induction plasma deposition, metallic bipolar plate, near-net-shape forming, solid oxide fuel cell, spray angle, vacuum plasma spraying

1. Introduction

Fuel cells convert the reaction energy of hydrogen or other fuels with oxygen directly into electrical energy. The oxidation of the fuels occurs in two steps at two electrodes, which are separated by a gas-tight, ion-conducting electrolyte. The electrons are exchanged via an external circuit where electrical energy can be obtained. The different types of fuel cells are characterized by the electrolyte material and their typical working temperature (Ref 1). In solid oxide fuel cells (SOFC) the electrolyte is a ceramic, usually yttria-stabilized zirconia (YSZ) that requires operating temperatures of approximately 950°C to ensure an appropriate ion conductivity.

Solid oxide fuel cells promise high efficiencies at electricity generation together with a very high utilization value of the primary (chemical) energy, because the high temperature level of the waste heat of the SOFC eases its use for further processes. Several geometrical designs of SOFCs are pursued, at present, where planar designs seem to have the best potential to achieve high power densities (Ref 2, 3). In such a design the single cells are electrically connected in parallel and in series by bipolar

plates to offer as a stack usable voltage and power values. These interconnects are the supporting parts, and they also distribute and separate the fuel and oxidant gases (Fig. 1).

According to their multiple function, the bipolar plates must be gas-tight, electrically and thermally conductive, mechanically stable, and corrosion resistant under oxidizing and reducing conditions at temperatures up to 1000°C .

Several materials, for example ceramics, cermets, and metals, were considered for the required properties of the bipolar plate. An alloy consisting of 94 wt% chromium, 5 wt% iron, and 1 wt% yttria was specially developed for this application by Plansee AG, Reutte/Austria (Ref 4). The bipolar plates made from this alloy have the advantage of very good performance, but their drawbacks are their mechanical properties. The coefficient of

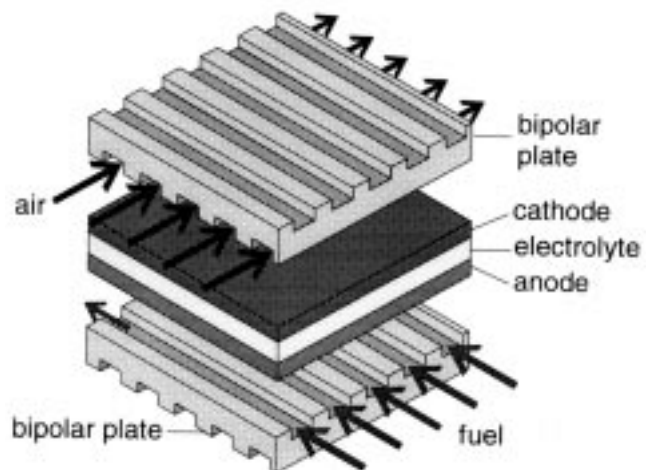


Fig. 1 Schematic of a single cell in a planar solid oxygen fuel cell with a cross flow arrangement of the fuel and the oxidant gas

B. Henne, M. Müller, and G. Schiller, Deutsches Zentrum für Luft- und Raumfahrt (DLR), Institut für Technische Thermodynamik, Pfaffenwaldring 38-40, D-70569 Stuttgart, Germany; E. Proß, H.C. Starck GmbH & Co. KG, D-79725 Laufenburg, Germany; and F. Gitzhofer and M. Boulos, Département de Génie Chimique, Université de Sherbrooke, Sherbrooke (Québec), J1K 2R1 Canada.

thermal expansion is very well adapted to that of the other cell components, and the electrical and thermal conductivities of the alloy are reasonably high. The material is stable in the long term, is gas-tight, and does not conduct oxygen ions. However, the metallic plates have a quite high temperature for ductile-to-brittle transition (200 to 450 °C), bear high residual stresses, and have a low notch impact strength (Ref 4, 5). A problem is the formation of volatile chromium oxides and hydroxides at the air side at high operating temperatures (Ref 6, 7). Vacuum plasma spraying of a protective layer onto the bipolar plates proved to be successful in solving this problem (Ref 8).

Currently the metallic bipolar plates are manufactured by a rather time consuming and complicated process. This process includes the mechanical alloying of the material, the shaping of green bodies and their sintering under hydrogen atmosphere, the encapsulation (“canning”) of the resulting parts for forging and rolling to achieve full density, the removal of the cans, and eventually, the production of the gas access holes and the gas channels by water jet cutting and electrochemical machining (ECM), respectively (Ref 4). Besides improving this production route, other methods with the potential to become less expensive and less time consuming should be introduced to meet the economical requirements of the SOFC production.

Induction plasma spraying, based on developments of Reed in the early sixties (Ref 9) and on improvements in the meantime with respect to knowledge and technology (Ref 10-12), promises to have the required potential for the required production cost reduction. The principle of a radio frequency (RF) induction plasma torch is used for the experiments of this study, as shown in Fig. 2.

The intrinsic properties of RF plasma have been used to produce the metallic bipolar plates for planar SOFCs. The electrodeless plasma generation diminishes the probability of contamination of the deposited material compared to the more conventional direct current (DC) plasma spraying. The large volume and low velocity of the RF plasma jet compared to DC plasma spraying result in a long dwell time of the particles in the plasma (10 to 20 ms) and, thus, allow the melting of even coarse

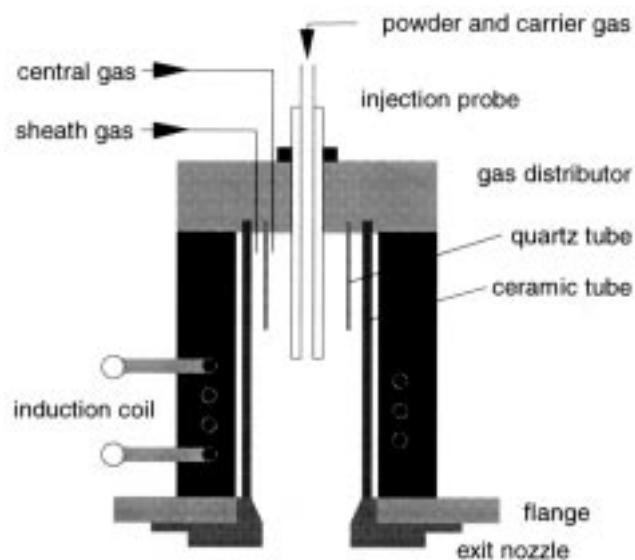


Fig. 2 Principle of an induction plasma torch

material at high throughput, such as recycled material of used bipolar plates prepared by grinding. Such a material cannot easily be resintered or recycled in another way for bipolar plates.

Furthermore, it should be discovered whether the material can be processed as near as possible to the final shape of the bipolar plates by spraying it onto contoured substrates. At this point, a major disadvantage of the RF plasma spray technique becomes obvious: the fixed installation of the relatively large torch. It will be necessary to spray the material onto the slopes of the bipolar plate structure under off-normal spray angles. The microstructure of coatings plasma sprayed onto inclined surfaces was studied by a few research groups who found a strong dependence of the quality on the incidence angle (Ref 13, 14). The behavior of materials sprayed onto macrostructured substrates is described in Ref 15.

2. Experimental Procedures

2.1 Materials

Two different powders of the composition 94 wt% Cr, 5 wt% Fe, and 1 wt% Y_2O_3 were used: (a) a mechanically alloyed pow-

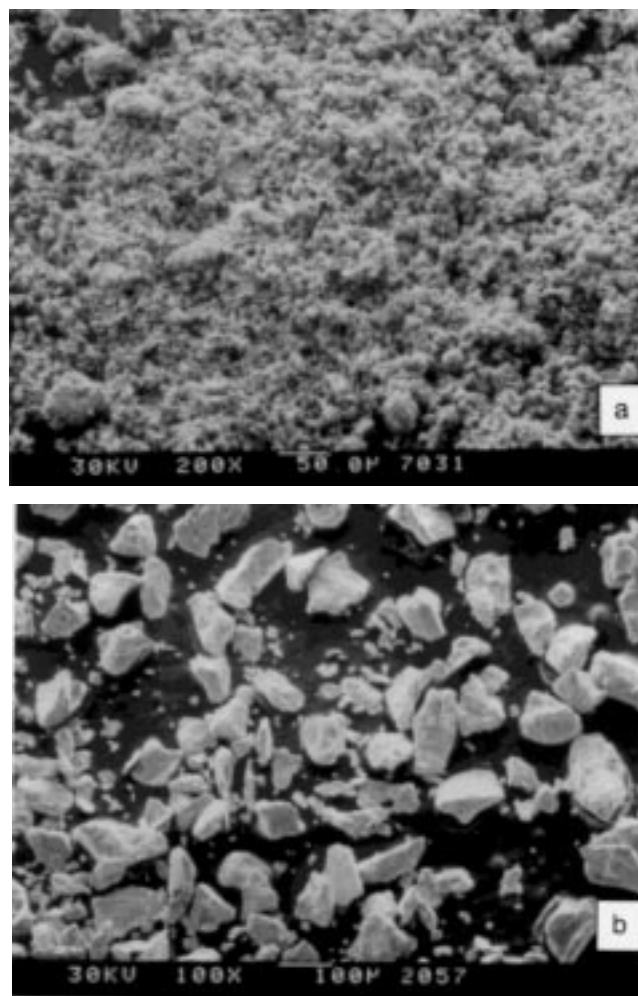


Fig. 3 Grain sizes and morphologies of the powders applied. (a) Mechanically alloyed. (b) Recycled by grinding of used bipolar plates

der as applied for the conventional production of bipolar plates by sintering methods at Plansee AG and (b) a recycled powder produced by grinding of sintered parts. The recycled powder

Table 1 Optimized process parameters

Parameter	Range	Mechanically alloyed powder	Recycled powder
Sheath gas, slpm, Ar/H ₂	100/5-120/10	120/10	120/10
Central gas, slpm, Ar	36-50	50	40
Plate power, kW	20-100	75	50
Preheating time, s	0-120	120	120
Spray distance, mm	150-250	200	150
Probe-nozzle distance, mm	45-75	45	45
Powder feed rate, g/min	20-80	40	40

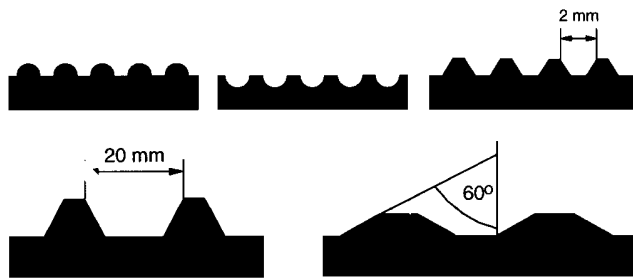


Fig. 4 Some of the substrate geometries applied

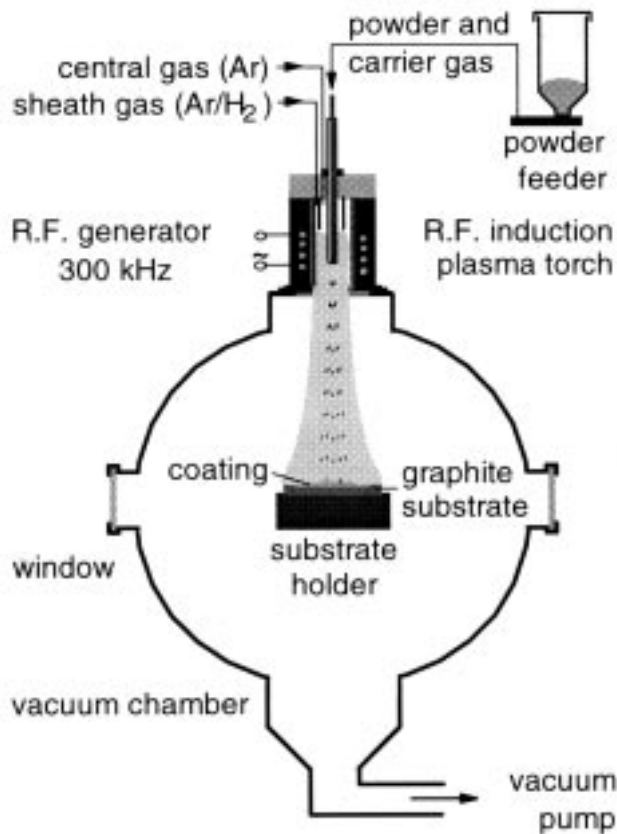


Fig. 5 Schematic of the experimental setup

was screened to use only the grain size fraction $<90\ \mu\text{m}$. The median grain size of the mechanically alloyed powder was $7\ \mu\text{m}$. For comparison, Fig. 3 shows the grain morphologies of the two powders.

2.2 Spraying Procedures

For the ease of the fabrication of a structured surface, graphite substrates were chosen for the first attempts. The powders were sprayed onto planar substrates of $70\ \text{by}\ 70\ \text{by}\ 10\ \text{mm}^3$ size, positioned with incidence angles of 90° and 45° with respect to the plasma jet axis and onto substrates of $50\ \text{by}\ 50\ \text{by}\ 10\ \text{mm}^3$ size, with negative shapes of potential bipolar plate designs. Enlarged graphite models of negative shapes of such designs were introduced to study the effects of off-normal incidence angles and of the transition areas of different angles on one substrate (Fig. 4). All substrates were coated with boron nitride prior to the experiment to ease the separation of substrate and deposit in order to obtain free-standing metal plates.

The experiments were performed in a vacuum reactor at the Centre de Recherche en Technologie des Plasmas (CRTP) at the Université de Sherbrooke in Canada using a PL70 induction plasma torch from TEKNA Plasma Systems Inc., Sherbrooke, Canada (Fig. 5). The system was operated with an oscillator frequency of approximately 300 kHz. The chamber pressure was kept constant at 200 torr (27 kPa). The powder was injected using argon with a constant carrier gas flow rate of 4 slpm. Other dominant process parameters were varied in the range given in Table 1.

2.3 Deposit Analysis and Sample Preparation

The resulting deposits were evaluated for surface roughness and deposition efficiency. With optimized conditions (Table 1), deposition efficiencies of approximately 70% and a high surface smoothness of the deposit were achieved. After each run the deposit was separated from the substrate and then cut for metallographic preparation. The embedded and polished cross sections were electrolytically etched in 10% nitric and 5% acetic acid for better observation of the splat shape. Porosity measurements were performed at the cross sections using image analysis software KS 300 from Kontron Elektronik, München, Germany.

3. Results and Discussion

3.1 Porosity

Three types of pores can be detected in the micrographs: (a) large angular pores, (b) elongated pores situated between splats, and (c) small spherical pores ($<1\ \mu\text{m}$), which are similar to pores of a sintered material. The porosity increases close to the substrate. This emphasizes the importance of strong preheating to obtain the requested flattening of the particles striking the substrate, if, what can be expected, the experiences with DC plasma spraying (Ref 16) are true also for the induction plasma method.

The results and micrographs presented in the following belong to samples sprayed with the recycled powder. For the finer mechanically alloyed powder, comparable tendencies were observed but on a lower porosity level. Figure 6(b) demonstrates

the feasibility of near-net-shape production of free-standing deposits of the chromium alloy by RF plasma spraying, but it also depicts the limits of this method to produce shaped bodies (Fig. 6a) in the case of the enlarged graph in model substrates (like Fig. 4d and e). The samples sprayed with an incidence angle of 30° (between plasma jet axis and substrate surface) show even macroscopic porosity, as can be easily seen in Fig. 6(a). In contrast, with an angle of 60° , optical microscopy is needed to find fine pores in the deposit (Fig. 6b).

Figure 7 shows the dependence of the porosity on the spray angles, as measured by image analysis of the cross sections shown in Fig. 8, where at a fixed parameter set “enlarged” substrate contours were used.

Figure 8 depicts the increase of porosity with decreasing spray angles for the deposits produced with the recycled powder. Not only the total porosity, but also the pore size increases. A typical phenomenon, which can be observed in samples sprayed under spray angles deviating from 90° , is that the pores combine to form pore channels (Fig. 8b-d). This leads to alternating dense and highly porous areas, resulting in rough surfaces, as was reported in Ref 13.

In contrast to Fig. 8(a), where even at an incidence angle of 90° some porosity with isolated pores can be observed, very dense metallic plates with porosities of less than 1% can be produced at this angle when the spray conditions are carefully chosen. Figure 9 gives an example of a very dense plate sprayed with recycled powder under optimized conditions.

It is an interesting phenomenon that porosities with acceptable low values can also be obtained for spray angles considerably deviating from 90° (Fig. 6c) when finely structured substrates corresponding to Fig. 4 are used. Obviously the appearance of pore channels is not only dependent on the incidence angle but also on the dimensions of the substrate contours to be replicated.

3.2 Shape and Arrangement of the Splats

The arrangement of the splats in deposits sprayed with an incidence angle of 90° was horizontal unless the splats surrounding particles either did not completely melt during their dwell in the plasma or were already resolidified at the moment of impact and appear now as spheres. The large pores were always in contact with such particles. The splat structure of the samples sprayed with the mechanically alloyed powder was finer compared to those of the recycled powder according to the grain size of the powders. The influence of the spray angle on the splat arrangement was identical for the two powders concerning the tendency. For simplicity reasons and because of the greater economical interest, the effects will be described only for the samples with the recycled powder.

There are only small differences detectable comparing the splat arrangement of the 90° samples with the 60° samples. At near normal incidence the splats usually followed the inclination so they were parallel to the surface, as was already reported in Ref 13. Figure 10(a) shows the transition from the splat arrangement parallel with the 90° surface to parallel with the 60° surface.

At shallow incidence angles the splat surfaces can no longer follow the inclined surfaces (Fig. 10b). The splats are bent and orientated almost perpendicular to the plasma jet direction. The splats of the 45° and 30° samples are arranged in columns, which

are perpendicular to the orientation of the splat surfaces (Fig. 8c, d and 10b). Smith et al. (Ref 13) explain that this microstructure was caused by the variation of the amount of material deposited in a given microscopic region according to the orientation of the splat surfaces in microscopic scale. A preferential deposition of the droplets on the regions, which are more perpendicular to the plasma jet, (e.g., higher points and the correlated lower deposition of material in the shadow of those high points), led to an unequal growth of neighbored, differently orientated regions (Ref

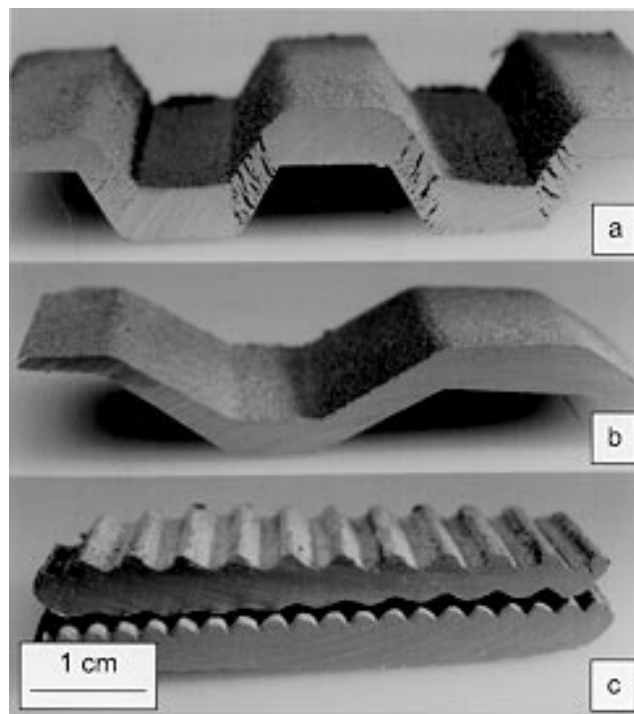


Fig. 6 Radio frequency plasma deposited free-standing parts of bipolar plate material. (a) Made with a geometrically extended contour of the substrate (removed), incidence angle at the flanks of 30° (with respect to the direction of the jet). (b) Like (a), but with an incidence angle of 60° . (c) Made with a finer substrate contour

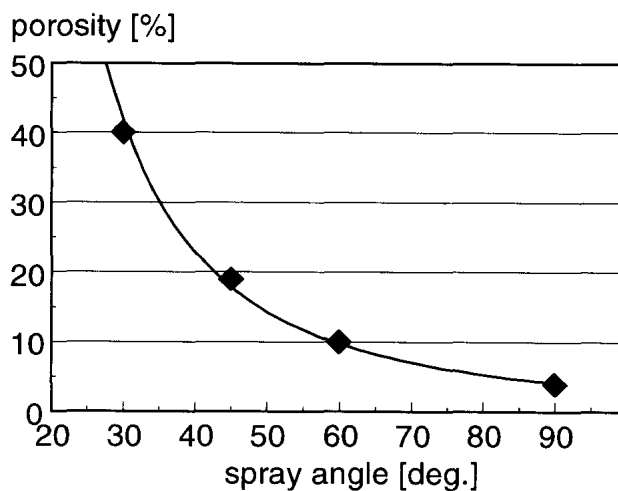


Fig. 7 Dependence of the porosity on the spray angle for “enlarged” substrate contours

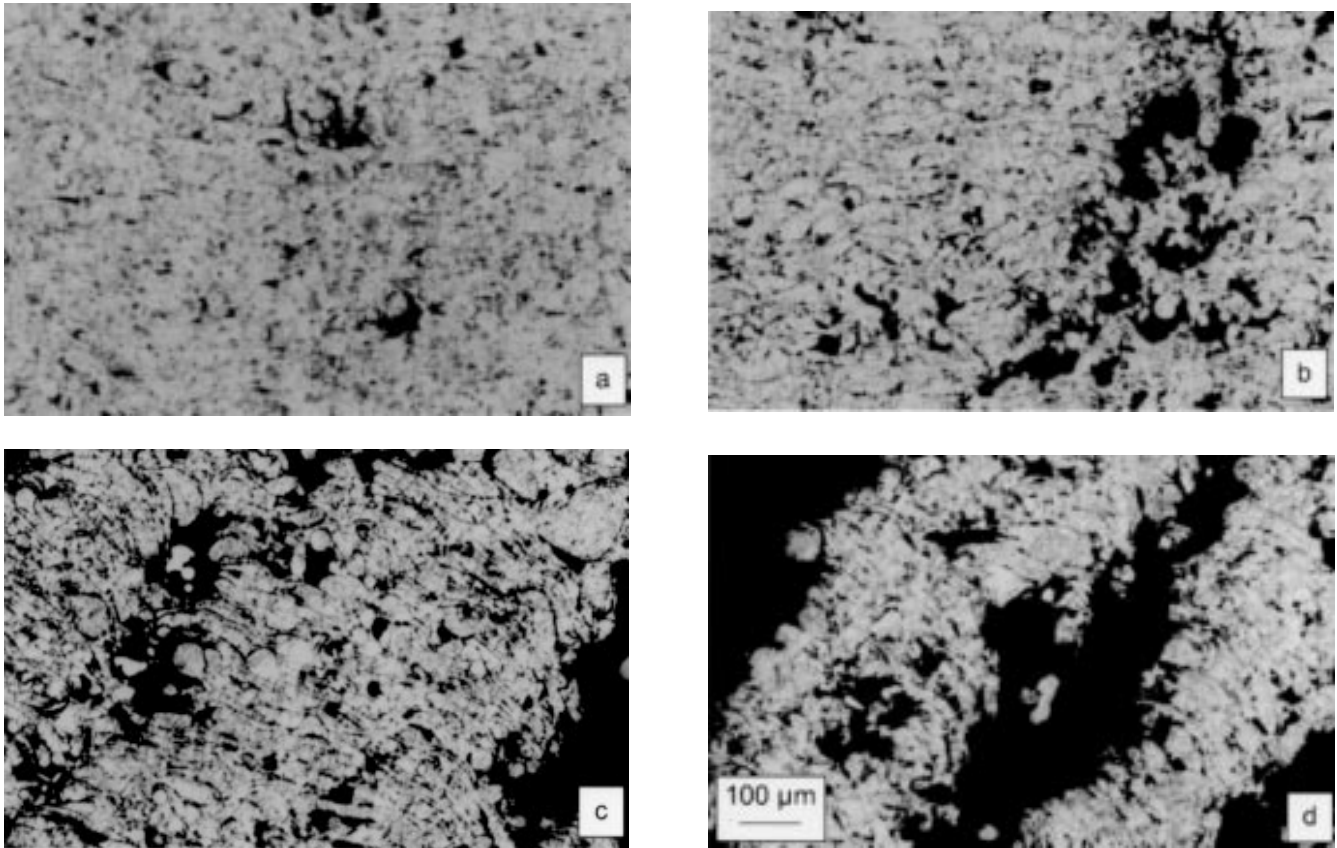


Fig. 8 Micrographs of etched cross sections of samples sprayed with recycled powder under different incidence angles. (a) 90°. (b) 60°. (c) 45°. (d) 30°

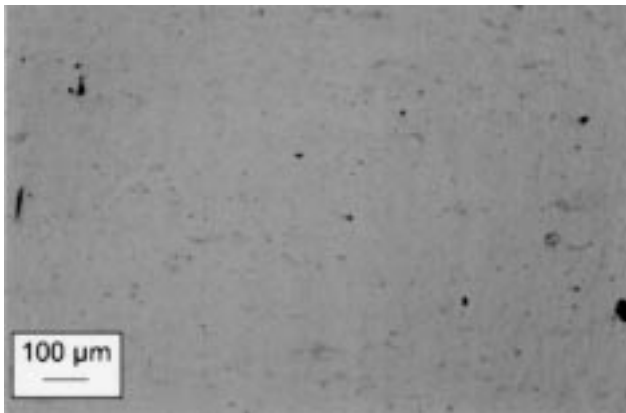


Fig. 9 Optical micrograph of a deposit with low porosity (approximately 1%)

13). In addition to the reasons for the column formation suggested by Smith et al., another effect might contribute to the process. The droplets striking the inclined substrate surface kept flowing downstream for a very short time and finally resolidified with an uneven thickness (Fig. 11). The subsequently impinging splat resolidified with a thicker downhill end, resulting in a gradual increase of the incidence angle at this position. Eventually a column grew with its single splats at a surface that was almost perpendicular to the spray axis. In the shadow of each column remained a pore channel. Pore channels and splat columns alternated along the inclined surface. The process

might be supported by a shearing of the deposited material as a result of gas dynamic forces. Figure 10 shows the beginning effect of column formation below the 90°C to 30°C edge in Fig. 10(b). In summary, the formation of such gas channels is highly detrimental for the requested gas tightness of the bipolar plates; therefore, means need to be developed to obtain tight layers even at inclined substrate surfaces.

3.3 Purity

Chemical analysis of some deposits performed at Plansee AG revealed deviations from the requested purity. This was mainly due to the materials applied for the substrate (graphite) and the separating layer (boron nitride). The highly detrimental influence of the nitride formation in a chromium lattice is discussed in Ref 5. The plasma spray process caused only minor changes in the yttria content of the mechanically alloyed powder. It should be positively mentioned that there was almost no increase in the oxygen content between the standard powder (0.42%) and a deposit produced with recycled powder (0.51%).

4. Conclusions

The present work demonstrated that the material of metallic bipolar plates for solid oxide fuel cells—a chromium alloy with the composition 94% Cr, 5% Fe, and 1% Y_2O_3 —can be processed by induction plasma spraying to almost dense, free standing

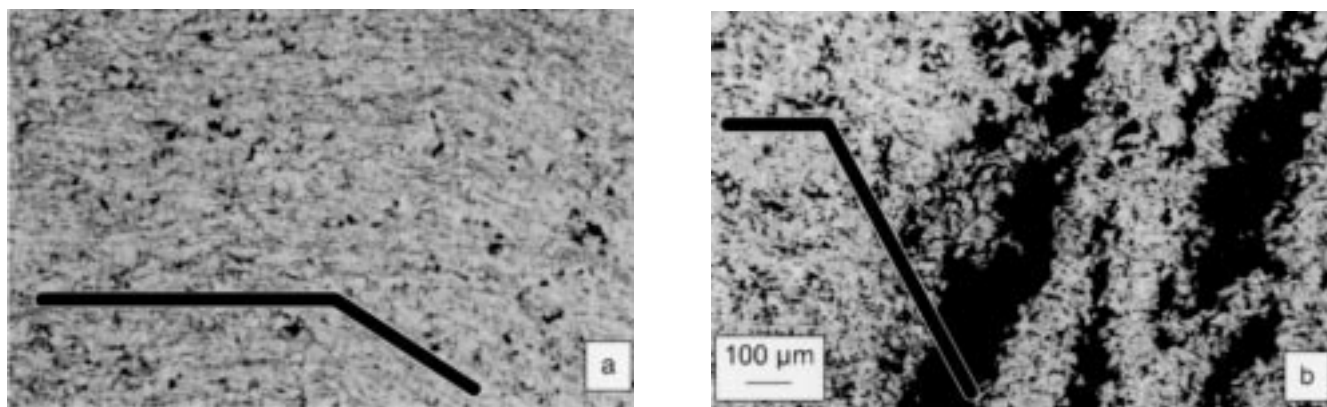


Fig. 10 Optical micrographs of etched cross sections depicting the transition areas from (a) 90 to 60° incidence angle and (b) 90 to 30°. The orientation of the substrate is indicated by the black bars.

parts. It should be emphasized that this is also possible with recycled material made by grinding of used plates. Such a material cannot be used again by a new sintering process. These bipolar plates usually have channels at the surface for the distribution of the reaction gases. Therefore, an attempt has been made to develop a near-net-shape deposition process by replicating the contours of “negatively” shaped graphite substrates, which were previously coated with a separating layer to ease the production of free-standing parts. It turned out that the quality of the deposits particularly at the channel flanks is not only dependent on the incidence angle, the angle between the jet direction, and the surface to be coated, but also on the width and depth of these channels. Whereas, with a grooved substrate with characteristic channel dimensions in the range of 1 or 2 mm, almost dense replicas can be obtained even at the critical zones where the incidence angle deviates considerably from normal; this is not possible at larger dimensions. Then, beginning with an incidence angle of about 60°, the formation of channels by interconnected pores appears with increasing tendency at decreasing incidence angle. In this case, to obtain dense or at least gas-tight deposits, a continuous periodic tilting of the substrate with respect to the spray jet direction could be helpful.

Furthermore, from the deposits obtained it can be positively concluded that, as long as the deposit thickness does not exceed about half the characteristic substrate dimension, the contour of the free side of the deposit sufficiently follows the contour of the substrate. This eases, for example, an economical production of channel plates for co- or counter-flow of fuel gas and air on either side of such new-type bipolar plates (Ref 17).

References

1. W. Drenkhahn, K. Hassmann, and H.-M. Kühne, Future Technology Fuel Cell and Battery, *Brennst.-Wärme-Kraft*, Vol 43 (No. 9), 1991, p 424-431 (in German)
2. N.Q. Minh and T. Takahashi, Stack Design and Fabrication, *Science and Technology of Ceramic Fuel Cells*, Elsevier, Amsterdam, 1995, p 233-306
3. J. Douglas, Solid Future in Fuel Cells, *EPRI J.*, March 1994, p 6-13
4. W. Köck, H.-P. Martinz, H. Greiner, and M. Janousek, Development and Processing of Metallic Chromium Based Materials for SOFC Parts, *Solid Oxide Fuel Cells IV*, Vol 95 (No. 1), M. Dokiya, O. Yamamoto, H. Tagawa, and S.C. Singhal, Ed., 1995, p 841-849
5. M. Janousek, Microstructure and Deformation Behavior of Powder Metallurgical Chromium Base Alloys between Room Temperature and 1100 °C in Dependence on the Production Technology, *VDI Fortschrittberichte*, Reihe 5 (No. 476), VDI Verlag GmbH, Düsseldorf, Germany, 1997 (in German)
6. K. Hilpert, D. Das, M. Müller, D.H. Peck, and R. Weiß, Chromium Vapor Species over Solid Oxide Fuel Cell Interconnect Materials and Their Potential for Degradation Processes, *J. Electrochem. Soc.*, Vol 143 (No. 11), 1996, p 3642-3647
7. C. Günther, H.J. Beie, P. Greil, and F. Richter, Parameters Influencing the Long Term Stability of the SOFC, *Proc. 2nd European Solid Oxide Fuel Cell Forum*, Vol 2, B. Thorstensen, Ed., Dr. U. Bossel, Oberrohrdorf, CH, Oslo, Norway, 1996, p 491-501
8. B. Brückner, C. Günther, R. Ruckdäschel, E. Fendler, and H. Schmidt, Improvement of the Long Term Stability in the High Temperature Solid Oxide Fuel Cell Using Functional Layers, *Proc. of 1996 Fuel Cell Seminar*, A. Pittman, Ed., Orlando, USA, 1996, p 155-158
9. T.B. Reed, Induction Coupled Plasma Torch, *J. Appl. Phys.*, Vol 32, 1961, p 821-824

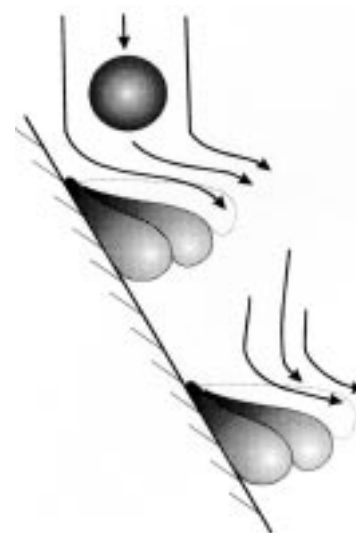


Fig. 11 Scheme of the beginning splat column formation at an inclined substrate. The gas flow is characterized by the black arrows.

10. M.I. Boulos, Inductively Coupled R.F. (Radio Frequency) Plasma, *Pure & Appl. Chem.*, Vol 57 (No. 9), 1985, p 1321-1352
11. M.I. Boulos, RF Induction Plasma Spraying: State-of-the-Art Review, *J. Therm. Spray Technol.*, Vol 1 (No. 1), 1992, p 33-40
12. M.I. Boulos, The Inductively Coupled Radio Frequency Plasma, *High Temp. Mater. Process.*, Vol. 1 (No. 1), 1997, p 17-39
13. M.F. Smith, R.A. Neiser, and R.C. Dykhuizen, An Investigation of the Effects of Droplet Impact Angle in Thermal Spray Deposition, *Thermal Spray Industrial Applications*, C.C. Berndt and S. Sampath, Ed., ASM International, 1994, p 603-608
14. G. Montavon, C. Coddet, S. Sampath, H. Herman, and C.C. Berndt, Vacuum Plasma Spray Forming of Astroloy: An Investigation of Processing Parameters, *Thermal Spray Industrial Applications*, C.C. Berndt and S. Sampath, Ed., ASM International, 1994, p 469-475
15. F. Bordeaux, R.G. Saint-Jacques, C. Moreau, S. Dallaire, and J. Lu, Thermal Shock Resistance of TiC Coatings Plasma-Sprayed on Macroroughened Substrates, *Thermal Spray Coatings: Properties, Processes, and Applications*, T.F. Bernecki, Ed., ASM International, 1991, p 127-134
16. S. Kuroda, T. Dendo, and S. Kitahara, Quenching Stress in Plasma Sprayed Coatings and Its Correlation with the Deposit Microstructure, *J. Therm. Spray Technol.*, Vol 4 (No. 1), 1995, p 76-84
17. R. Henne, E. Fendler, M. Müller, M. Boulos, and F. Gitzhofer, Procedure for the Manufacture of Shaped Bodies, European Patent 97102995.4-2307, 1997 (in German)